International Journal of Science and Research (IJSR)
ISSN: 2319-7064
Impact Factor 2025: 7.089

Effect of End Restraint and Global Slenderness on Buckling Behaviour of CFS Unequal-Leg Lipped Angle Columns

Sruthi P. V.

M. Tech. in Structural Engineering, Department of Civil Engineering, Rajadhani Institute of Engineering and Technology (Autonomous), Nagaroor, Attingal, Thiruvananthapuram, Kerala, India

Abstract: ***Cold-formed steel (CFS) unequal-leg lipped angle columns are thin-walled, monosymmetric members that may exhibit local, global and interaction buckling under axial compression. Their strength is sensitive to the restraint provided at the member ends. This Phase I study develops and validates a nonlinear finite element model of a CFS unequal-leg lipped angle column and uses it to examine the preliminary influence of end restraint. The reference specimen, 1.0-P-1, has leg dimensions of 115 mm and 105 mm, 15 mm return lips, a thickness of 1.0 mm and a length of 700 mm. The steel is represented using an elastic–perfectly plastic model with Young's modulus of 203,000 MPa, yield strength of 321.08 MPa and Poisson's ratio of 0.30. The column is modelled in ABAQUS using S4R shell elements. Linear eigenvalue buckling analysis is followed by geometrically nonlinear Static Riks analysis. The finite element peak load of 24.12 kN is compared with the experimental reference value of 23.00 kN, giving a difference of 4.87%. For the 700 mm column, the predicted ultimate loads are 24.12 kN, 18.99 kN and 16.67 kN for fixed-fixed, semi-rigid and pinned-pinned end conditions, respectively. The results indicate a clear reduction in load-carrying capacity as end restraint decreases. The effect of column length/global slenderness is included in the planned parametric programme; however, corresponding numerical results are not reported in the available Phase I material.***

Keywords: Cold-formed steel, unequal-leg lipped angle, end restraint, buckling, finite element analysis

1. Introduction

Cold-formed steel members are widely used in lightweight structural systems because of their high strength-to-weight ratio, fabrication efficiency and versatility. Unequal-leg lipped angle sections are used in bracing systems, trusses and lightweight frames. Their thin plate elements and unsymmetrical cross-sections make their compressive response sensitive to local plate instability and overall member buckling.

Under axial compression, local buckling may interact with flexural or flexural–torsional buckling. In unequal-leg sections, local deformation can shift the effective centroid and influence the subsequent global response. The restraint provided by end connections also affects the effective buckling length and the load at which instability develops. In practical structures, connections may provide partial rather than ideal fixed or pinned restraint.

The present Phase I work focuses on establishing a finite element modelling procedure for a CFS unequal-leg lipped angle column and examining the effect of end restraint for a 700 mm reference member. The wider project considers global slenderness by varying column length; the supplied report identifies lengths of 500, 700 and 900 mm for this purpose.

2. Literature Review

Umaraj et al. [1] investigated the structural behaviour and design of CFS unequal-leg lipped angle columns under axial compression using experiments, finite strip analysis and numerical validation. Their results identified local–global interaction buckling, in which local buckling influenced the centroid and triggered overall instability. They also reported that idealized fixed-end assumptions may not fully represent the restraint achieved in tests.

Young and Ellobody [2] examined the design of cold-formed steel unequal-angle compression members, while Young and Chen [3] reported column tests on non-symmetric lipped angle sections. These studies provide a basis for understanding the stability behaviour and design of thin-walled unequal-leg members. Ananthi [4] investigated cold-formed steel compound angle sections under axial compression and reported changes in failure behaviour with member slenderness and section geometry.

Recent work by Li et al. [5] on Q1100 ultra-high-strength unequal-leg angle stub columns reported combined local and torsional buckling. Thangavel et al. [6] investigated inward-lipped angle sections with triangular brackets and showed that added restraint can alter the governing failure mode. Other studies on cold-formed steel members have highlighted the importance of nonlinear modelling, connection representation and member slenderness [7]–[9].

2.1 Research Gap

The supplied literature review indicates that the behaviour of CFS unequal-leg lipped angle columns has mainly been examined under idealized end conditions. The influence of semi-rigid and pinned-pinned restraints, particularly when combined with changes in global slenderness, remains insufficiently quantified for the selected section. The present work addresses this gap through a nonlinear finite element framework and a preliminary comparison of three end-restraint conditions.

3. Objectives and Scope

The objectives of the study are: (i) to investigate the influence of end restraint on the buckling behaviour of CFS unequal-leg lipped angle columns; (ii) to examine the influence of global slenderness on ultimate strength and failure mode; and (iii) to study the combined influence of end restraint and global slenderness on interaction buckling.

The Phase I model is based on specimen 1.0-P-1 reported by Umaraj et al. [1]. The analysis considers concentric axial compression and three end conditions: fixed-fixed, semi-rigid and pinned-pinned. The project plan also specifies column lengths of 500, 700 and 900 mm. Distortional buckling as a separate design investigation, residual stresses, dynamic loading, embossed sections and multi-member assemblies are outside the stated scope.

4. Finite Element Modelling

4.1 Reference Specimen and Geometry

The reference member is a CFS unequal-leg lipped angle column designated 1.0-P-1. Its longer leg is 115 mm, shorter leg is 105 mm, return lip is 15 mm, plate thickness is 1.0 mm and reference length is 700 mm. The section was created in ABAQUS/CAE as a three-dimensional deformable shell profile. The thickness was assigned as a shell section property. Reference points were placed at the two ends and coupled to the end nodes to facilitate the application of boundary conditions and axial displacement.

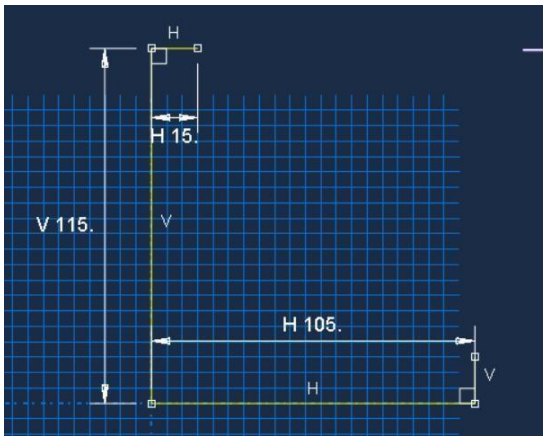


Figure 1: Cross-sectional dimensions of the reference unequal-leg lipped angle section

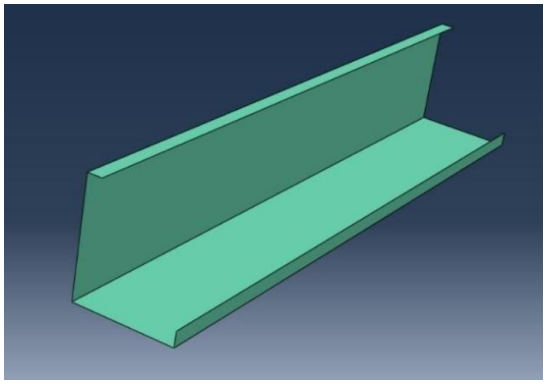


Figure 2: Three-dimensional shell model of the CFS column

Table 1: Geometric and material properties of specimen 1.0-P-1.

Parameter	Value
Longer leg, b_1	115 mm
Shorter leg, b_2	105 mm
Return lip	15 mm
Thickness, t	1.0 mm
Reference length, L	700 mm
Yield strength, fy	321.08 MPa
Young's modulus, E	203,000 MPa
Steel grade	G300

4.2 Material Model

The steel was represented using an elastic–perfectly plastic constitutive model. The Young's modulus was taken as 203,000 MPa, the yield strength as 321.08 MPa and Poisson's ratio as 0.30. The report also lists an ultimate strength of 411 MPa. The elastic–perfectly plastic idealization was used to represent the elastic stiffness and yielding response in the nonlinear analysis.

Table 2: Material properties used in the finite element model

Property	Symbol	Value
Young's modulus	E	203,000 MPa
Poisson's ratio	ν	0.30
Yield strength	fy	321.08 MPa
Ultimate strength	fu	411 MPa

4.3 Element Type and Mesh

The column was discretized using four-node reduced-integration shell elements (S4R). These elements were selected to represent the membrane and bending behaviour of the thin-walled section while capturing local and global instability. A mesh-size study was reported for 20, 15, 10, 7.5 and 5 mm. The report selected a 10 mm mesh as a balance between computational effort and accuracy.

Table 3: Mesh-size study values transcribed from the report

Mesh size (mm)	Peak load (kN)
20	30.97
15	20.08
10	26.45
7.5	27.83
5	30.87

Note: the source report contains a discrepancy for the 15 mm result (20.08 kN in the table and 26.08 kN in the plotted graph). In addition, the listed peak loads do not show a clearly converged trend from 10 mm to 5 mm. The mesh-convergence data should therefore be rechecked against the original ABAQUS output before journal submission.

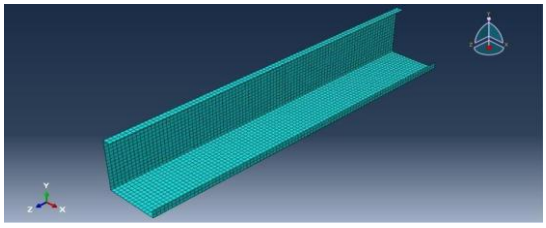


Figure 3: Meshed finite element model of the CFS column

4.4 Boundary Conditions and Loading

Reference points at both ends were coupled to the corresponding end regions. For validation, a fixed-fixed configuration was used. The base reference point was restrained in all six degrees of freedom, while the top reference point was restrained against rotation and lateral movement and subjected to axial displacement. The parametric comparison considered fixed-fixed, semi-rigid and pinned-pinned end conditions. The semi-rigid condition was represented by an intermediate effective-length factor.

4.5 Analysis Procedure

A two-stage analysis procedure was adopted. First, a linear eigenvalue buckling step (Buckle) was used to obtain elastic critical loads and corresponding mode shapes. The first eigenmode was then used to inform the geometric imperfection pattern for the nonlinear model. Second, a geometrically nonlinear Static Riks analysis was performed to trace the equilibrium path beyond the peak load and obtain the ultimate load and post-buckling response.

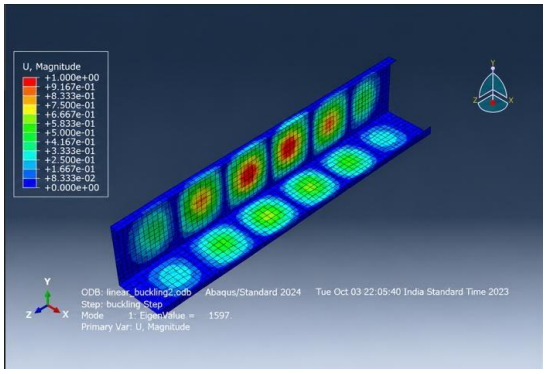


Figure 4: Representative linear eigenvalue buckling mode shape

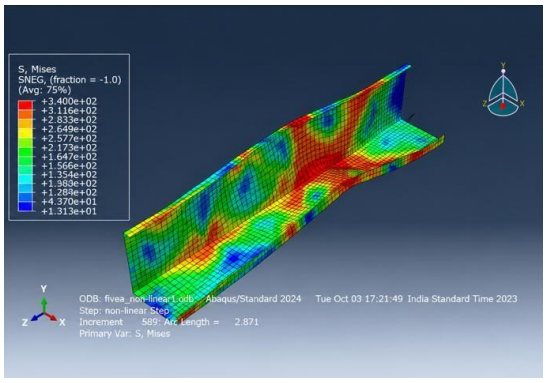


Figure 5: Representative nonlinear buckling deformation pattern

5. Model Validation

The finite element model was compared with the experimental peak load reported for specimen 1.0-P-1 by Umaraj et al. [1]. The experimental value adopted in the validation table is 23.00 kN, while the present finite element model predicts 24.12 kN. The percentage difference is calculated as:

Percentage difference = $|24.12 - 23.00| / 23.00 \times 100 = 4.87\%$

Table 4: Comparison of experimental and finite element peak loads

Parameter	Experimental [1]	Present FEM	Difference
Peak load (kN)	23.00	24.12	4.87%

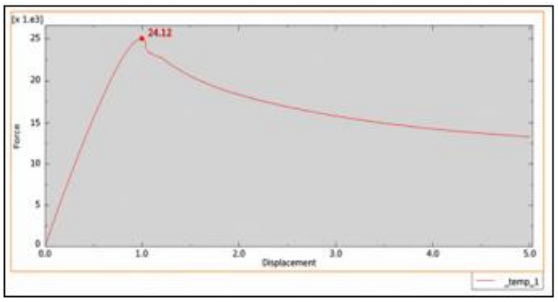


Figure 6: Load–displacement response obtained from the finite element analysis.

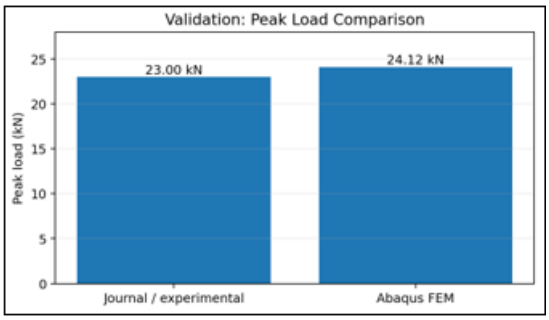


Figure 7: Comparison of experimental and finite element peak loads.

The finite element prediction is 4.87% higher than the experimental value. The report attributes the difference mainly to the idealized rigid end restraint in the numerical model, the absence of residual stresses and the use of an assumed first-eigenmode imperfection instead of measured specimen imperfections. The value 24.12 kN is used consistently here because it is the value in the report's validation table and conclusion.

6. Preliminary Parametric Study: End Restraint

For the preliminary end-restraint comparison, the column length was held constant at 700 mm. The fixed-fixed condition was assigned an effective length of 350 mm (K = 0.5), the semi-rigid condition an effective length of 490 mm (K = 0.7), and the pinned-pinned condition an effective length of 700 mm (K = 1.0). Linear buckling analysis was followed by nonlinear Riks analysis for each condition.

Table 5: Buckling and ultimate loads for the 700 mm column

End condition	Effective length factor, K	Pcr (kN)	Pult (kN)
Fixed-fixed	0.5	15.98	24.12
Semi-rigid	0.7	13.05	18.99
Pinned-pinned	1.0	12.01	16.67

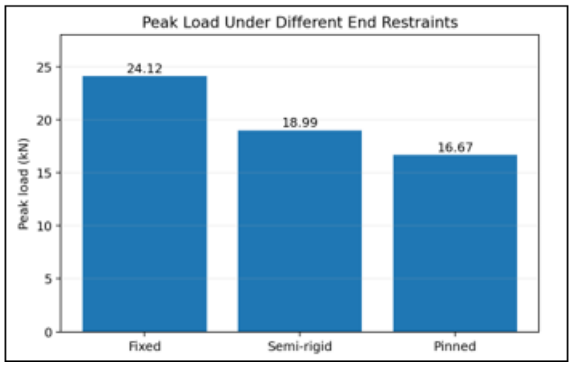


Figure 8: Ultimate load comparison for the three end-restraint conditions.

The ultimate load decreases as the end restraint is reduced: 24.12 kN for fixed-fixed, 18.99 kN for semi-rigid and 16.67 kN for pinned-pinned support. The fixed-fixed model therefore carries approximately 44.69% more load than the pinned-pinned model, based on (24.12 − 16.67)/16.67 × 100. The report describes local–global interaction buckling in all three cases and notes that deformation increases as the end restraint decreases. The fixed-fixed case exhibits the highest stiffness, whereas the pinned-pinned case reaches instability at the lowest load.

7. Global Slenderness: Phase I Status

The project plan identifies three member lengths—500, 700 and 900 mm—to investigate global slenderness under each of the three end-restraint conditions, giving nine planned analysis cases. The available Phase I report provides the parametric matrix but does not include numerical results for all three lengths or a completed comparison of the corresponding slenderness effects. Accordingly, no quantitative conclusion on the influence of global slenderness is claimed in this manuscript. Completion of the nine-case nonlinear analysis is required before drawing conclusions on the combined effect of end restraint and global slenderness.

8. Conclusions

A nonlinear finite element model of a CFS unequal-leg lipped angle column was developed in ABAQUS using S4R shell elements and a two-stage eigenvalue/nonlinear Riks analysis procedure. For the reference specimen, the predicted peak load of 24.12 kN differed from the reported experimental value of 23.00 kN by 4.87%.

For the 700 mm member, end restraint had a marked influence on ultimate load. The predicted capacities were 24.12 kN, 18.99 kN and 16.67 kN for fixed-fixed, semi-rigid and pinned-pinned conditions, respectively. The fixed-fixed condition provided approximately 44.69% greater capacity than the pinned-pinned condition. These Phase I results demonstrate the importance of representing end restraint when modelling the stability of thin-walled unequal-leg lipped angle columns.

The planned investigation of global slenderness through 500, 700 and 900 mm member lengths remains to be completed. The mesh-convergence values and the 15 mm mesh result also require verification from the original analysis files before final journal submission.

References

[1] R. R. Umaraj, S. K. Selvaraj, and T. M. Chan, “Structural behaviour and design of cold-formed steel unequal-leg lipped angle columns,” Engineering Structures, vol. 341, Art. no. 120789, 2025.
[2] B. Young and E. Ellobody, “Design of cold-formed steel unequal angle compression members,” Thin-Walled Structures, vol. 45, no. 3, pp. 330–338, 2007.
[3] B. Young and J. Chen, “Column tests of cold-formed steel non-symmetric lipped angle sections,” Journal of Constructional Steel Research, vol. 64, nos. 7–8, pp. 808–815, 2008.
[4] G. B. G. Ananthi, “A study on cold-formed steel compound angle section subjected to axial compression,” KSCE Journal of Civil Engineering, vol. 22, no. 5, pp. 1803–1815, 2018.
[5] S. Li, X. Xue, F. Wang, T. M. Chan, and B. Young, “Behaviour of cold-formed Q1100 ultra-high strength steel unequal-leg angle section stub columns,” Thin-Walled Structures, Art. no. 114290, 2025.
[6] P. Thangavel, M. Palanisamy, W. Wipulanusat, and K. Roy, “Investigation of a cold-formed steel inward lipped angle section with triangular brackets under compression: Numerical and theoretical investigations,” Structures, vol. 79, Art. no. 109404, 2025.
[7] A. Singh, Z. Zhang, X. Wang, B. W. Schafer, and T. C. Hutchinson, “Practice-oriented numerical model for seismic response of cold-formed steel-framed mid-rise buildings,” Engineering Structures, vol. 319, Art. no. 118833, 2024.
[8] L. Bai, J. Yang, and M. A. Wadee, “Cellular buckling from nonlinear mode interaction in unequal-leg angle struts,” Thin-Walled Structures, vol. 132, pp. 316–331, 2018.
[9] J. F. Zhang et al., “Eccentric compressive distortional buckling and design of non-symmetric cold-formed angular column with complex edges,” Thin-Walled Structures, vol. 165, Art. no. 107981, 2021.